



## Article

# Application of Indoor Greenhouses in the Production of Thermal Energy in Circular Buildings

Eusébio Conceição <sup>1,2,\*</sup> , João Gomes <sup>3</sup>, Maria Inês Conceição <sup>4</sup> , Margarida Conceição <sup>4</sup>, Maria Manuela Lúcio <sup>1</sup> and Hazim Awbi <sup>5</sup>

<sup>1</sup> Faculdade de Ciências e Tecnologia, Universidade do Algarve, Campus de Gambelas, 8005-139 Faro, Portugal; maria.manuela.lucio@gmail.com

<sup>2</sup> ADAI, Departamento de Engenharia Mecânica, Rua Luís Reis Santos, Pólo II, 3030-788 Coimbra, Portugal

<sup>3</sup> CINTAL, Campus de Gambelas, 8005-139 Faro, Portugal; jgomes@ualg.pt

<sup>4</sup> Instituto Superior Técnico, Universidade de Lisboa, 1049-001 Lisboa, Portugal; ines.conceicao@tecnico.ulisboa.pt (M.I.C.); margarida.conceicao@tecnico.ulisboa.pt (M.C.)

<sup>5</sup> School of Built Environment, University of Reading, Reading RG6 6AW, UK; h.b.awbi@reading.ac.uk

\* Correspondence: econcei@ualg.pt

## Abstract

The production of thermal energy in buildings using internal greenhouses makes it possible to obtain substantial gains in energy consumption and, at the same time, contribute to improving occupants' thermal comfort (TC) levels. This article proposes a study on the producing and transporting of renewable thermal energy in a circular auditorium equipped with an enveloping semi-circular greenhouse. The numerical study is based on software that simulates the building geometry and the building thermal response (BTR) numerical model and assesses the TC level and indoor air quality (IAQ) provided to occupants in spaces ventilated by the proposed system. The building considered in this study is a circular auditorium constructed from three semi-circular auditoriums supplied with internal semi-circular greenhouses. Each of the semi-circular auditoriums faces south, northeast, and northwest, respectively. The semi-circular auditoriums are occupied by 80 people each: the one facing south throughout the day, while the one facing northeast is only occupied in the morning, and the one facing northwest is only occupied in the afternoon. The south-facing semi-circular greenhouse is used by itself to heat all three semi-circular auditoriums. The other two semi-circular greenhouses are only used to heat the interior space of the greenhouse. It was considered that the building is located in a Mediterranean-type climate and subject to the typical characteristics of clear winter days. The results allow us to verify that the proposed heating system, in which the heat provided to the occupied spaces is generated only in the semi-circular greenhouse facing south, can guarantee acceptable TC conditions for the occupants throughout the occupancy cycle.

**Keywords:** building geometry; building thermal response; circular auditorium; semi-circular auditorium; thermal comfort; indoor air quality; semi-circular greenhouses



Academic Editors: Christian Inard and Boris Igor Palella

Received: 31 December 2024

Revised: 16 July 2025

Accepted: 17 July 2025

Published: 24 July 2025

**Citation:** Conceição, E.; Gomes, J.; Conceição, M.I.; Conceição, M.; Lúcio, M.M.; Awbi, H. Application of Indoor Greenhouses in the Production of Thermal Energy in Circular Buildings. *Energies* **2025**, *18*, 3962. <https://doi.org/10.3390/en18153962>

**Copyright:** © 2025 by the authors. Licensee MDPI, Basel, Switzerland. This article is an open access article distributed under the terms and conditions of the Creative Commons Attribution (CC BY) license (<https://creativecommons.org/licenses/by/4.0/>).

## 1. Introduction

### 1.1. Context

Currently, climate change, mainly due to the increase in greenhouse gas emissions of anthropogenic origin, has caused a significant increase in the external ambient temperature and the concentration of carbon dioxide (CO<sub>2</sub>) in the atmosphere. Consequently, this has been one of the most significant factors that have contributed to the conditions for

establishing adequate levels of thermal comfort (TC) and indoor air quality (IAQ) in the occupied interior spaces of buildings, increasingly demanding [1,2]. Consequently, more and more buildings are resorting to the systematic use of mechanical heating, ventilation, and air-conditioning (HVAC) systems, which also requires a systematic and increasing use of energy to power these systems [3,4]. This impact on energy consumption is reflected in energy demand in the buildings sector, accounting for more than 35% of global energy use and more than 38% of reported CO<sub>2</sub> emissions [5]. In order to reduce this impact, with regard to HVAC systems, efforts have been made to make these systems more efficient, using, for example, new methods [6] or more effective control strategies [7]. In Europe, the construction sector has been moving towards making buildings nearly zero energy use [8,9]. There are several options to achieve this objective: use of diverse sources of renewable energy; increase the energy efficiency of the building; and reduce the use of fossil energy [10]. Santos-Herrero et al. [11] present a review article focused on strategies used, such as the contribution of the building envelope or passive solutions implemented, in the types of HVAC systems (with emphasis on the use of renewable energy sources or heat pumps and the type of emitter) and the way the building's energy management is carried out (using a wireless sensor network, or the application of predictive control models or simulation programs), among other issues. Another aspect to highlight is the influence that occupancy has on the energy performance of the building, so its modeling must always be considered and carefully defined [12]. Also, passive building concepts, close to zero energy use, can contribute to a significant reduction in greenhouse gas emissions during their life cycle, according to the study conducted by Maierhofer et al. [13]. Hybrid solutions, involving the building envelope and the integration of photovoltaic systems, such as those proposed in Masi et al. [14], contribute to achieving positive balances between the energy savings obtained and the environmental performance verified. In Portugal, Resende and Corvacho [15] showed that using only passive solutions, some thermal discomfort is observed; however, it is possible to achieve adequate levels of thermal comfort if, in addition, equipment that consumes energy from renewable sources is used, thus effectively reducing the energy consumption of HVAC systems powered by the electricity grid. Some studies show that the use of passive green glass space (GGS) technology has the potential to achieve a positive balance between thermal comfort and energy savings [16,17]. GGS is a transitional space made up of a glass facade separating the exterior and interior environments. In winter conditions, this space can provide heat for heating interior spaces. The study developed by Xi et al. [16] shows that it is possible to achieve savings in energy consumption of around 50% and, at the same time, maintain acceptable thermal comfort levels as shown by the results given by the indices used—air distribution performance index above 85% and percentage of dissatisfied below 1%. However, in summer conditions this system loses effectiveness and can lead to overheating, which is why Zhang et al. [17] propose to complement the GGS system with the use of cooled air from an underground tunnel connected to this system. In this way, it is possible to control the cooling loads by varying the airflow rate.

### *1.2. Buildings Geometry and Energy*

The building evaluated in this study resembles a real building on existing in a university campus located in the southern region of Portugal. The building has the geometry of a circular auditorium surrounded around the entire exterior perimeter by a corridor. This corridor is surrounded by a glazed surface that is exposed to solar radiation in a large part of its surroundings. The circular auditorium is made up of three independent semi-circular auditoriums. Each semi-circular auditorium is surrounded by the corresponding semi-circular portion of the corridor. This surrounding space, which is made up of

a corridor, allows the creation of a greenhouse area that will be used to heat the air that will be supplied to the auditoriums. In a passive way, especially in winter conditions, solar radiation can be a very important source of renewable energy when there are glazed surfaces that can receive it and allow it to be used in a very efficient way, depending on glazing materials [18], the presence of shading devices [18,19], the position and orientation of windows [20]. The amount of heating power due to solar radiation depends on external factors such as the level of solar insolation and the presence of clouds of dust pollution in the atmosphere [21]. However, other factors can influence the thermal behavior of the building, such as external environmental factors (air temperature and wind speed) and the behavioral attitudes of the occupants [21,22].

The type of space (auditorium) considered here is usually intended for theoretical classes, seminars, and conferences, being occupied by a large number of people, so this building must provide good thermal comfort, draught risk, indoor air quality, and acoustic conditions [23–26].

The geometric layout of this type of circular auditorium surrounded by a closed circular space whose outer surface is glazed and subject to the influence of incident solar radiation, which operates as an internal greenhouse that is used to convert solar radiation into thermal energy that will be used to heat occupied interior spaces in the winter season. The way in which this auditorium and its surrounding internal greenhouse were divided into three sets of semi-circular auditoriums plus semi-circular internal greenhouses allows thermal energy to be stored in a given space (the one subject to the highest levels of incident solar radiation) and that to be subsequently transported to other spaces. This thermal energy is transported by ducts when these spaces are not in contact or by open holes between the spaces when they adjoin each other. The geometry of this building was developed using a computational aided design (CAD) methodology. CAD methodologies are often applied in the most diverse building-related studies [27,28].

### 1.3. Internal Environmental Variables

The most relevant internal environmental variables used in the numerical study developed in this article are CO<sub>2</sub> concentration, indoor air temperature ( $t_a$ ), indoor air relative humidity (RH), mean radiant temperature ( $t_r$ ), and indoor air velocity ( $v_a$ ).

CO<sub>2</sub> concentration due to human activity is one of the most used contaminants in the assessment of IAQ in buildings [29–32], with values recorded in the occupants' breathing zone being particularly important [33]. IAQ depends on the air ventilation rates implemented in the space occupied [34–36], so well-designed ventilation systems must be in place. In most school buildings, IAQ can be effectively improved using natural ventilation [37,38]. In order to maintain adequate IAQ levels, ASHRAE Standard 62.1 [39] specifies the minimum air change rate depending on the type of building, the volume of the space to be ventilated, and the airflow rate required per person (i.e., in function of occupation). This standard also proposes an acceptable IAQ limit for a CO<sub>2</sub> concentration of up to 700 ppm above outdoor air level [39]. The European standards, ISO 17772 [40,41] and EN 16798 [42,43], indicate specific limits for CO<sub>2</sub> concentration according to the different Indoor Environmental Quality categories, which can vary between 550 ppm and 800 ppm above the external CO<sub>2</sub> concentration level. In line with European standards, the Portuguese standard on ventilation requirements and indoor air quality, Portaria n° 353-A/2013 [44], indicates 1250 ppm as an acceptable limit for IAQ.

TC is influenced by indoor environmental parameters such as  $t_a$ , RH,  $t_r$ , and  $v_a$ . To obtain acceptable TC conditions, standards such as ASHRAE 55 [45] and ISO 7730 [46] suggest requirements for the predicted mean vote (PMV) and predicted percentage of dissatisfied (PPD) thermal comfort indexes, indoor operative temperature, and indoor air relative

humidity. PMV and PPD indexes were established by Fanger [47]. Zomorodian et al. [48] refer to several models for evaluating thermal comfort in educational buildings, where it was shown that rational and adaptive models are mostly used to evaluate TC in classrooms accurately. However, the PMV index continues to be applied in the assessment of thermal comfort [49–51]. It is commonly considered that the PMV index does not adequately predict thermal comfort in naturally ventilated buildings [52,53]. However, Alfano et al. [54] concluded that it is also possible to effectively use the PMV index in the assessment of TC in naturally ventilated compartments if an expectancy factor is applied. It is important to note that it is necessary to continue to develop more accurate thermal comfort models that can overcome the limitations of both adaptive and static models. In this sense, thermo-physiological models [55,56], which provide precise thermal comfort predictions across a wide range of microclimatic conditions and which have been validated based on a wide set of experimentally obtained data, are a good example of a line of research to follow.

#### *1.4. Numerical Models*

In the numerical analysis of the thermal behavior of buildings, it is essential to use software that effectively evaluates the performance of environmental variables inside buildings based on the establishment of external environmental conditions, including solar radiation, that reliably characterize the type of climate in which the building is located. In this work, proprietary software called building thermal response (BTR) is used, capable of simulating the thermal behavior of buildings with complex topologies, whose application with proven results can be observed, for example, among other recent works, in Conceição et al. [57]. The BTR software calculates the temperature and mass concentration distributions in the building, information that will allow the establishment of the TC and IAQ conditions observed in the various spaces that make up the building. This software was validated in steady-state and transient conditions, both in the cooling and heating seasons, in school buildings and experimental chambers [58]. The use of numerical programs in the analysis of the thermal behavior of buildings has been fundamental in research, as demonstrated, for example, by the studies carried out by Picallo-Perez et al. [59], Fawwaz Alrebei et al. [60] and Diz-Mellado et al. [61].

#### *1.5. Contributions and Objectives*

On the way to making buildings with energy balances close to zero and, therefore, more sustainable because they also contribute to reducing greenhouse gas emissions, the use of renewable energy is fundamental. The southern region of Portugal has high levels of solar radiation, with normal direct irradiation values between 5.02 and 5.90 kWh/m<sup>2</sup> [62], which justifies its use as a resource to be used, for example, passively for heating buildings in the winter season. In this region, there is a university building with a circular structure consisting of a set of auditoriums with a semi-circular geometry, surrounded by an accessible closed space whose surroundings have glazed surfaces around its entire perimeter. This building, thus, presents constructive characteristics that allow a greenhouse to be created between the auditoriums and the external glazed envelope in order to take advantage of solar radiation, incident on most of its surroundings, to heat the air to be introduced into the occupied spaces by the ventilation system during the winter season. In order to assess its potential for use and consequent energy savings by avoiding the use of HVAC systems, a prior numerical study must be carried out.

The BTR software used in this study to simulate the thermal response of buildings has been developed by the authors over the last three decades and offers a significant set of added value. This software incorporates a set of innovative models and allows communication with a set of upstream software (which operate as inputs) and a set of

downstream software (which operate as outputs). Therefore, the BTR software, which works like a virtual laboratory, allows us to develop innovative work in the most diverse areas (passive uses for cooling and heating indoor environments, new HVAC systems, dual-skin facades, among many others).

The BTR software consists of a set of models that, in a transient regime, allow the calculation of, among others, the following:

- A system of integral equations for energy and mass balance, based on the geometry of the building, which is automatically generated by the software itself;
- A set of temperatures in opaque, transparent and interior bodies as well as in interior spaces;
- A set of concentrations of water vapor as well as a set of concentrations of different contaminants emitted inside the space and entering it;
- Direct and diffuse solar radiation on different surfaces;
- Internal and external shading based on the distribution of the building's own surfaces and those of others located nearby;
- The different convective phenomena by natural, forced and mixed convection occurring on vertical, horizontal and inclined surfaces;
- The different conductive phenomena depending on the different compositions of the building bodies;
- The radiative properties of glass;
- Internal radiation exchanges;
- The levels of indoor thermal comfort and indoor air quality.

It is worth noting that the BTR software also considers the simulation of internal duct systems.

In terms of inputs, the BTR software communicates with other software that generates input data, such as external environmental variables, solar radiation, building geometry, internal ventilation, occupancy, and others. In this work, the software that generates the building surfaces presents significant added value, both in terms of increasing the speed of design by automatically generating the building's geometry, even complex geometries such as that of the building under study here, and in the ability to implement changes to its geometry in a short period of time. Regarding its outputs, the BTR software communicates, for example, with the software used in the application of thermal response and human thermophysiology to perform detailed calculations of thermal comfort levels, with the Computer Fluid Dynamics software, to perform detailed calculations of air quality inside spaces, and with the software that allows acoustic studies to be carried out in indoor spaces, among others.

The major contribution of this article is the development of the software used here to optimize the design of a passive building so that it achieves its best possible thermal performance. Thus, this study is carried out using two coupled software programs, one that simulates the geometry of the building and the other that simulates the thermal response of the building. During the development process, the coupling between these two software programs allows the geometry of the building to be adjusted more functionally and quickly to the corresponding thermal response of the building, taking into account the desired level of thermal comfort. Another contribution to be highlighted is the implementation of circular internal greenhouses in this building. This circular indoor greenhouse, subject to incident solar radiation from sunrise to sunset, will be used to heat the building's internal spaces. Efficient management of the use of thermal energy produced throughout the day in these circular greenhouses and efficient distribution of the hot air stored there through a well-designed ventilation system will provide better thermal comfort conditions for the occupants.

Following the work carried out in Conceição et al. [63], where a numerical model was developed that allows the design of this type of circular building, the objectives of the work presented in this article are as follows:

- Develop a thermal system, in a circular auditorium, in winter conditions, that can guarantee good TC and IAQ conditions for its occupants, throughout most of the day, using renewable energy, namely the passive use of radiation solar incident on a circular glazed enclosure of a space constituted as a greenhouse that surrounds this auditorium;
- Numerically evaluate the transient thermal response of the building mentioned above;
- As a result of the implemented system, characterize the TC and IAQ conditions provided to the occupants of this building by this passive solar heating system.

## 2. Models and Methods

### 2.1. Building Thermal Response

The numerical model applied in this work corresponds to that implemented in the BTR software, which the authors developed and upgraded over the years. The numerical model calculates the building's temperature and mass distribution and evaluates the TC and IAQ levels. It uses inputs from other software that generates the three-dimensional geometry of the auditoriums of the circular structure building and other inputs, namely, the external environmental conditions, geographical conditions, airflow rate distribution, and occupation distribution, among other variables.

The numerical model, used to evaluate the circular auditorium's thermal response, is created considering a set of convective, conductive, radiative, and evaporative phenomena in buildings. Therefore, it is constituted by [64,65]:

- Integral energy balance equations that allow the evaluation of the temperature field of a set of bodies (interior, opaque, and transparent) as well as indoor spaces;
- Integral mass balance equations that evaluate the mass field of a group of gases, such as water vapor and CO<sub>2</sub>.

The integral energy balance equations consider the accumulation of energy on the left side of the equation and the heat fluxes and generation on the right side of the equation. These equations consider heat fluxes by radiation, conduction, convection, and evaporation/condensation.

The heat flux by radiation is due to solar radiation and radiative exchanges. Using the BTR software, the direct and diffuse solar radiation incident on the building are calculated throughout the day for a specific location on the globe. In solar radiation, absorption in opaque bodies and absorption and transmission in transparent bodies are considered. In opaque bodies located inside the compartments and in internal bodies, the absorption of radiation that passed through the glass is considered. This transmission is calculated through the radiative properties of the glass, which take into account both the thickness and composition of the glass and the angle of incidence of solar radiation on the glass. Radiative exchanges within each space are calculated taking into account the shape factors between the different internal surfaces and the temperature of each of the surfaces.

The heat flux by radiation is considered in opaque bodies. This phenomenon takes into account the thermal properties and dimensions of the different layers of the opaque body. Thermal resistances in series and parallel are considered.

In opaque, transparent, and interior bodies, natural, forced, and mixed convection phenomena are considered on their different surfaces. These calculations are performed on horizontal, tilted, and vertical layers. In these calculations, dimensionless parameters are used to calculate the heat transmission coefficient.

Evaporation and condensation are considered on internal surfaces. In the evaluation of these phenomena, the mass transmission coefficients (also calculated in a dimensionless form) are considered, taking into account horizontal, tilted, and vertical surfaces.

Heat generation is carried out by the HVAC system and the occupants. In the case of the occupants, due to their physical activity, heat generation is always positive, contributing to an increase in the internal air temperature. In the case of the HVAC system, generation can be positive, when in heating mode, or negative, when in cooling mode.

The integral mass balance equations consider mass accumulation on the left side of the equation and mass fluxes and generation on the right side of the equations. In each space, convective fluxes, generation, and adsorption/desorption in opaque and transparent bodies are considered. Convection considers the flow that enters and leaves each space from the external environment, directly from other compartments, or from ventilation duct systems. The internal generation of water vapor and CO<sub>2</sub> is carried out through the bodies of the occupants and their respiratory systems. Adsorption/desorption is carried out on the internal surfaces of the opaque and internal bodies. Adsorption occurs when the internal concentration is higher in the internal space than in the bodies, and desorption occurs when the internal concentration is lower in the internal space than in the bodies.

The integral energy and mass balance equations systems are solved by the Runge–Kutta–Felberg numerical model with error control.

The geometry of the buildings is taken into account by the BTR software, namely:

- Occupied and non-occupied indoor spaces, such as the semi-circular auditorium and semi-circular greenhouse;
- Opaque bodies, such as the inside and outside walls, ceiling, and floor, among others;
- Transparent bodies, such as windows and other glazed surfaces;
- Inside bodies, such as the internal walls, pillars, furniture, among others.

The integral energy balance equations are generated for the following elements:

- Air inside spaces, whether occupied or not;
- Different layers of the opaque bodies;
- Transparent and inner bodies.

The integral mass balance equations are generated to evaluate the following:

- Adsorption and desorption of water vapor in opaque and inner bodies;
- Water vapor and the CO<sub>2</sub> concentration (or other contaminants) inside spaces, whether occupied or not.

The BTR software considers the following inputs:

- Building data, namely, the building geometry, the building materials' thermal properties, the occupation, and the ventilation;
- Geographical parameters, such as the Mediterranean environment in the South of Portugal at sea level;
- External environmental variables, such as the external AT, external air RH, and external wind speed, for a typical winter day (21 December).

The five days prior to the day to be evaluated are also simulated by the BTR software to allow the transient simulation results to stabilize, and balance is achieved with external environmental variables. This methodology is used to obtain the initial and boundary conditions. All variables taken into account at the beginning of the simulation are in balance with the environmental variables.

21 December was chosen because it is the day of the year in the region (Southern Portugal) where the study is being conducted that has the lowest number of sunlight hours. In studies involving the use of passive solar heating, this day is chosen because it is the one that, in clear sky conditions, will have the lowest amount of available solar radiation. A

good performance of the system under study on this day allows us to infer that, in similar clear sky conditions, the system will also have a positive performance on the other days of the winter season.

The model implemented here has some limitations in order to reduce calculation time while maintaining good accuracy of the results obtained. It is worth mentioning that the heat flow is unidirectional in walls, as well as in opaque and transparent bodies; the thermal variables of the interior air and of the interior bodies, are uniform and the radiative heat exchanges inside the space are not considered.

## 2.2. Building Geometry Generation

The circular auditorium geometry (CAG) software generates buildings with circular geometry. In this work, the building geometry (shown in Figures 1 and 2 with and without a roof, respectively) comprises three semi-circular auditoriums and respective surrounding greenhouses and identifies the building's materials. The CAG software is based on trigonometric geometric equations that consider cylindrical coordinates [63]. These equations consider the following: ceiling; floor; semi-circular greenhouses; side; stage; steps; wall surface; and window surface [63].

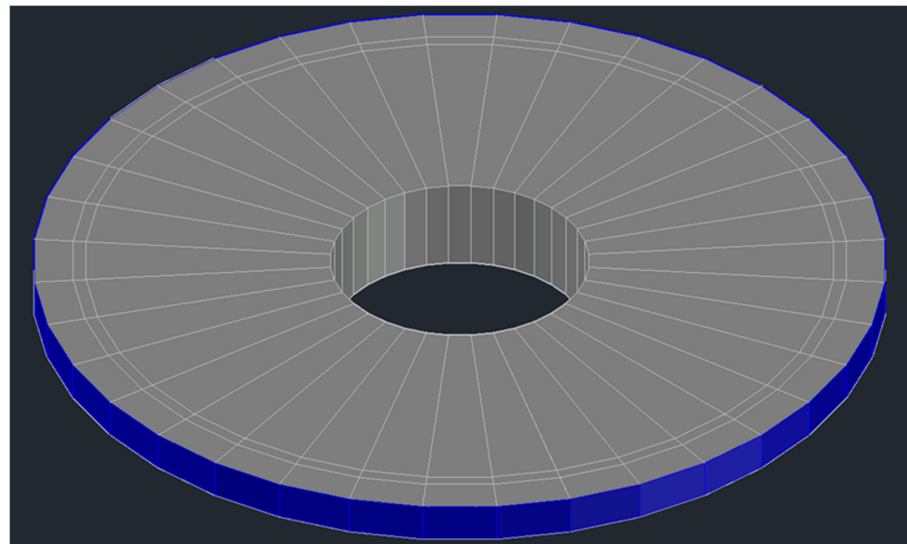


**Figure 1.** Building geometry, with a roof, considered in this study.

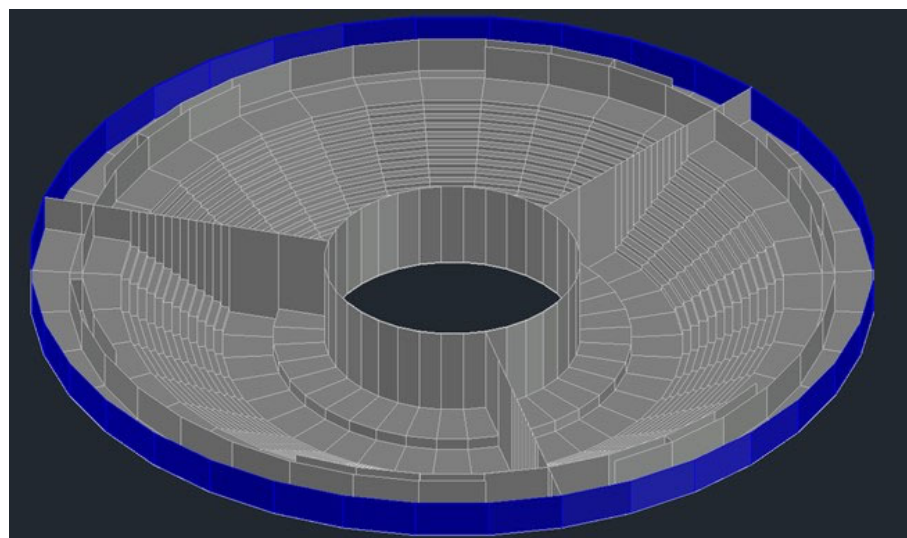


**Figure 2.** Building geometry, without a roof, considered in this study.

First, the number of auditoriums and the initial and final angles of each one are defined. The depth and initial and final radius of each auditorium must be taken into account. It is also important to consider the number of occupants, paying attention to the space allocated to the benches, staircase, and stage. The total height of the auditorium is also defined. In the upper internal area of the auditorium, the height of a space is established that will be reserved for ventilation systems and acoustic systems, among others.

The software starts by designing the stage, staircase, and benches, as well as the vertical surfaces on the sides and fronts. The front surfaces of the upper area include the entrance doors placed perpendicular to the walls. The internal greenhouse that surrounds the outside of the auditorium is also taken into account. In this case, the depth and height of this internal greenhouse must also be dimensioned. Finally, the roofs are designed according to a radial shape.

When transferring information between software, the composition of each surface, whether opaque, transparent, or internal, is also taken into account. This composition includes the type of layers in series and parallel, three-dimensional dimensions of the surfaces used in the calculation of incident solar radiation and shading, angles of the different surfaces used in the calculation of incident solar radiation, and spatial identification of adjacent compartments.

The output data of the CAG software is used as input data in:

- CAD software used to design the circular auditorium;
- BTR software used to simulate the circular auditorium thermal response.

The virtual circular auditorium consists of three equal semi-circular auditoriums surrounded by semi-circular greenhouses, as shown in Figures 3–5. These semi-circular auditoriums are numbered and oriented as follows:

- 2, northeast;
- 3, northwest;
- 4, south.

These surrounding semi-circular greenhouses are numbered and oriented as follows:

- 5, northeast;
- 6, northwest;
- 7, south.

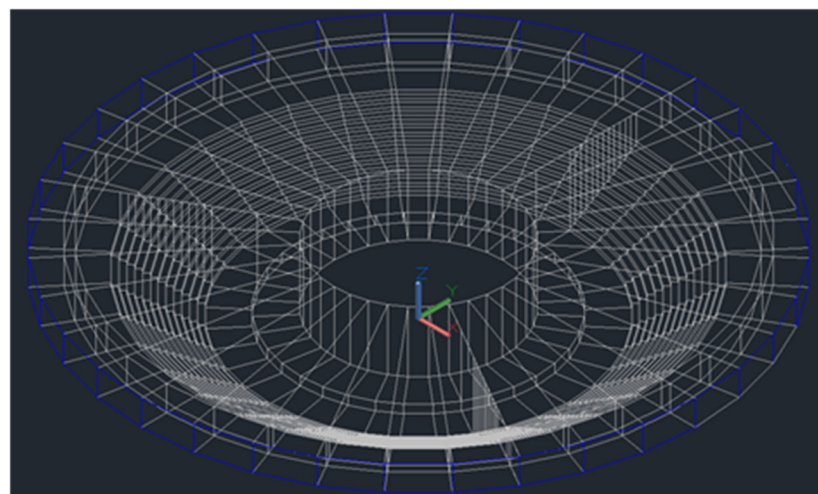


**Figure 3.** South-east view of the three-dimensional passive circular auditorium equipped with three semi-circular auditoriums, surrounded by three semi-circular greenhouses. X points to the east direction and Y points to the north direction.

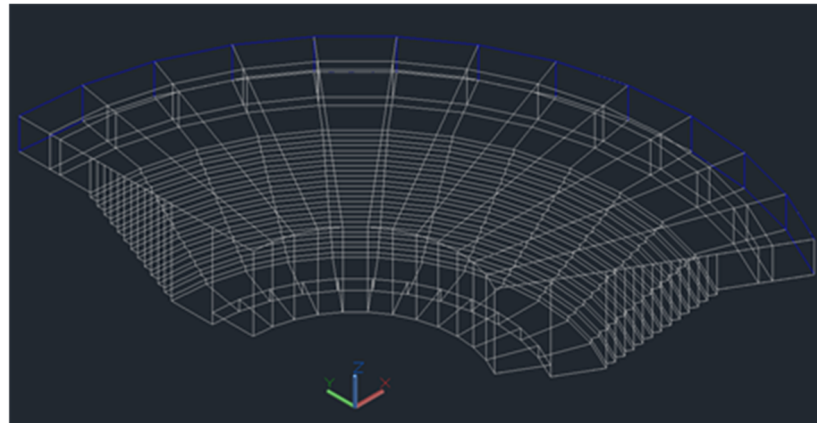


**Figure 4.** South-east view of the three-dimensional passive semi-circular auditorium, surrounded by a semi-circular greenhouse. X points to the east direction and Y points to the north direction.

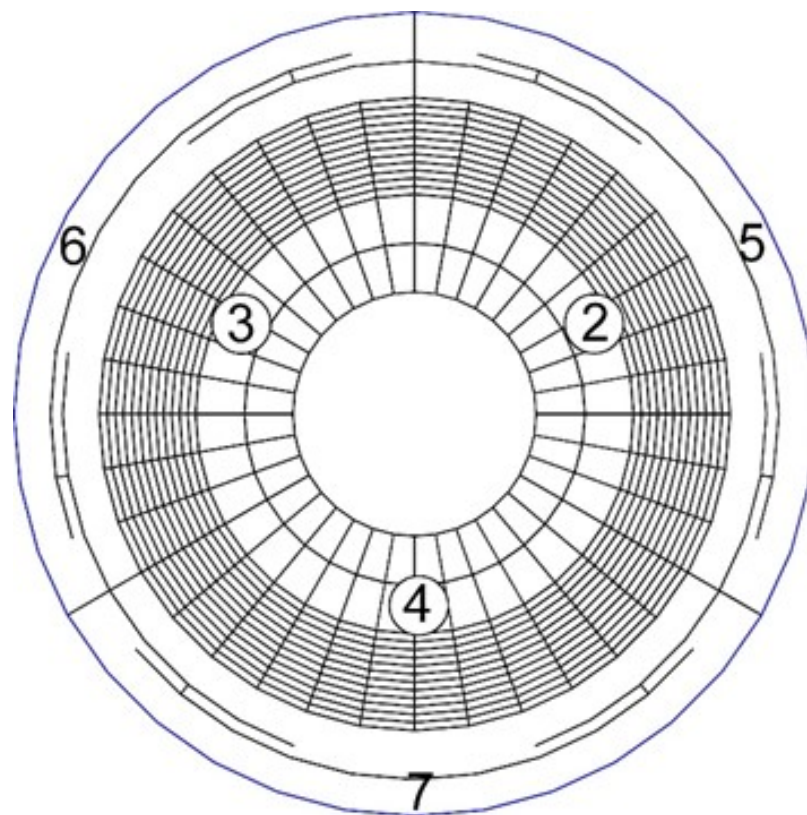


**Figure 5.** Top view of the three-dimensional passive circular auditorium with the numeration of the three semi-circular auditoriums (2 to 4), surrounded by three semi-circular greenhouses (5 to 7).

The circular auditorium consists of:

- Opaque surfaces: ceiling; doors; floor; interior walls made of simple brick; exterior walls made of double brick; stage; and steps.
- Thirty-six glazed surfaces heat the spaces inside the circular auditorium from the passive use of incoming solar radiation, available according to the sun's path throughout the day. Considering the counter-clockwise direction, the glazed surfaces per semi-circular are numbered as follows (see also Figure 6): 1 to 12 in semi-circular greenhouse 1; 13 to 24 in semi-circular greenhouse 2; 25 to 36 in semi-circular greenhouse 3.

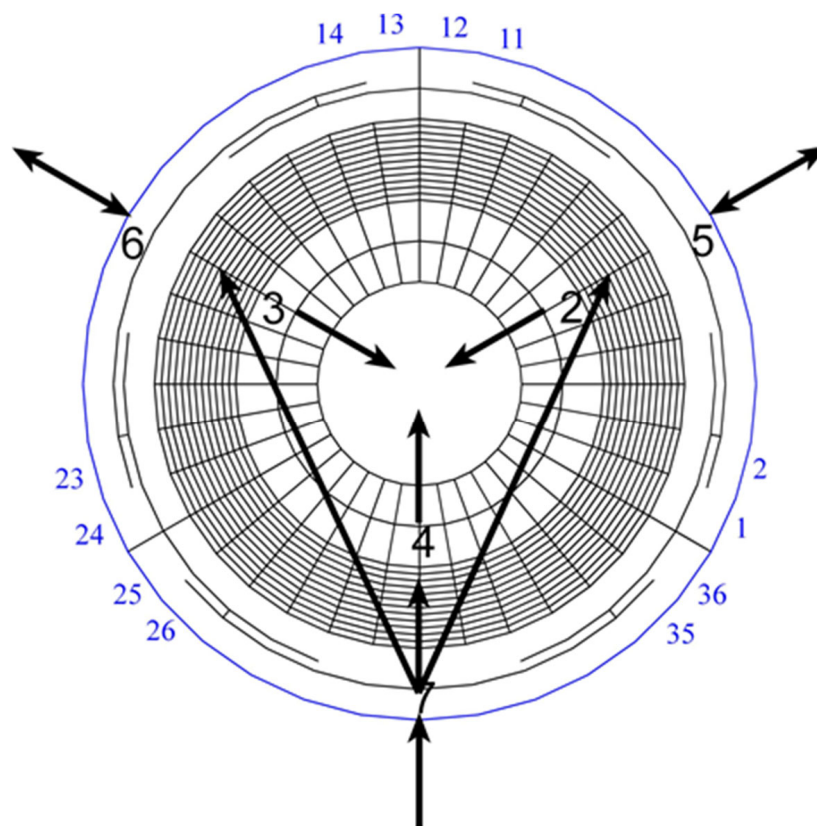


**Figure 6.** Airflow topology.

### 2.3. Efficient Use of Solar Heat Gains

The efficient use of solar heat gains is performed in the surrounding greenhouses by the accumulation of radiative heat in the air inside them and on their internal surfaces. Since the greenhouses are circular and surround the entire auditorium, solar radiation hits these greenhouses throughout the day from sunrise to sunset, which allows radiative heat to accumulate in their interior space throughout this period. The transport of the thermal energy accumulated in the air inside the surrounding circular greenhouses is performed by mechanical ventilation through the ducts that make up the ventilation system that supplies the circular auditorium.

### 2.4. Airflow Rate and Indoor Air Quality

The airflow rate used is shown in Table 1 and is in line with the Portuguese standard [44]. The ventilation system consists of fans installed at the entrance to the ducts that distribute air throughout the occupied spaces. These fans can be mechanically driven or electrically powered by photovoltaic panels with battery support. The ventilation system implemented is of the perfect mixing type. The inlet air temperature is that provided by the air temperature inside the surrounding circular greenhouses, and the inlet air speed depends on the airflow rate. The ventilation system ducts are connected between the surrounding circular greenhouses and the auditorium. Outside air is supplied through openings in the circular greenhouses by mechanical ventilation.

**Table 1.** Airflow rate [44].

Occupation	Ventilation
With occupation	35 m <sup>3</sup> /h by person
Without occupation	1 h <sup>-1</sup>

In this work, CO<sub>2</sub> concentration is used as the contaminant that characterizes IAQ [44]. IAQ is influenced by the ventilation system's airflow rate, volume, and number of occupants in the ventilated space. The considered value of external CO<sub>2</sub> concentration is 400 ppm.

The airflow topology, shown in Figure 6, is the one used by the ventilation system: the semi-circular greenhouse (number 7) in the semi-circular auditorium facing south is used to heat the three semi-circular auditoriums (numbers 2, 3, and 4). The semi-circular greenhouses facing northeast (number 5) and northwest (number 6) are used to heat the semi-circular greenhouse itself.

### 2.5. Occupation Distribution

The semi-circular auditoriums (2, 3, and 4) are occupied according to the distribution shown in Table 2. The occupation considered is 80 people. The occupancy depends on the geometry of the space and corresponds, most of the time, to the maximum occupancy values recorded in similar spaces in the region. Note that the semi-circular auditorium 4 (facing south) is occupied during the morning and afternoon, while the semi-circular auditorium 2 (facing northeast) is only occupied during the morning and the semi-circular auditorium 3 (facing northwest) is only occupied in the afternoon. The occupancy cycle is defined to take advantage of the distribution of incident solar radiation on the glazed surfaces of the surrounding greenhouses. In semi-circular auditorium 2, incident solar radiation is predominant during the morning; in semi-circular auditorium 3, incident solar radiation is predominant during the afternoon; while in semi-circular auditorium 4, incident solar radiation is predominant during a time period that varies between approximately 10 a.m. and approximately 4 p.m. The main idea is to optimize the airflow topology implemented in the ventilation system and, simultaneously, evaluate the performance of the ventilation system when subjected to a high thermal load in the occupied spaces.

**Table 2.** Occupation cycle in the semi-circular auditoriums.

Hours (h)	Semi-Circular Auditorium Number		
	2	3	4
8 → 12	80	0	80
14 → 18	0	80	80

The external environmental conditions typical of a Mediterranean-type climate in Southern Portugal in the winter season were implemented in the simulation work carried out.

Each usual occupant (mainly students or teachers) of this type of space (auditorium) presents an average winter season clothing level in the region of 1.2 clo [45].

### 2.6. PMV and Thermal Comfort

The occupants' TC level will be assessed by the PMV index [47], an index presents in the commonly used ASHRAE 55 [46] and ISO 7730 [45] standards. When calculating the PMV index, environmental and personal variables are taken into account:

- Environmental variables obtained inside the spaces:  $t_a$ ,  $v_a$ , RH and  $t_r$ ;
- Personal variables such as metabolic rate and clothing insulation level.

In the present work, as all occupants are seated in an auditorium, a metabolic rate of 1.0 met was considered as provided for by the ISO 7730 [45].

The mean radiant temperature,  $t_r$ , is determined approximately from the average temperatures of the floor, surrounding walls, and ceiling [66,67]. These temperatures are weighted considering the area corresponding to each of the surrounding surfaces, making

the emissivity value equal to one. The value thus obtained is representative of the estimated average of  $t_r$  in the center of the considered space.

With regard to thermal comfort, the ASHRAE 55 [46] and ISO 7730 [45] standards classify indoor spaces according to three categories (A, B, or C) depending on the value of the calculated PMV index. In this work, category C (whose PMV values vary between  $-0.7$  and  $+0.7$ ) [45], the least restricted, was used to evaluate thermal comfort in the interior space of the three semi-circular auditoriums.

Although the building does not use an HVAC system, the option to use the PMV index to assess thermal comfort in this building is justified by the fact that it uses a ventilation system to distribute the hot air generated in the greenhouses to the auditoriums during the period of occupation.

To verify whether the results obtained with the PMV index in the assessment of thermal comfort can be duly considered, the determination of the zone for adaptive comfort based on the operative temperature ( $t_{op}$ ) is also used. The evolution of  $t_{op}$  as a function of time and  $t_{op}$  as a function of outside temperature will be calculated for each auditorium, and its location in relation to the adaptive comfort zone will be analyzed.

From the conditions defined for naturally ventilated buildings, the applicable adaptive comfort zone was obtained considering the equations of the upper and lower limits of the  $t_{op}$ , both defined as a function of the mean outdoor temperature in the ISO 17772 standard [40]. These limits were considered for Category II of ISO 17772 [40]. The  $t_{op}$  in each auditorium is determined according to the equations presented in Haiying et al. [68]. A compilation and respective critical analysis of the standards on thermal comfort and IAQ can be consulted in Khovalyg et al. [69].

### 3. Results

In this section, results obtained by the BTR software will be presented. The external environmental variables, the solar radiation to which the semi-circular greenhouse glass surfaces are subjected, the IAQ level (using the  $CO_2$  concentration), the indoor  $t_a$ , the  $t_r$ , and the TC level (using the PMV and  $t_{op}$ ), are presented.

#### 3.1. External Environmental Variables

For a typical winter day in the southern region of Portugal, namely 21 December, the external environmental variables generated are as follows:

- External  $t_a$ , whose variation is between  $6.5$  °C (at 7:00 a.m.) and  $13.5$  °C (at 3:00 p.m.);
- External air RH, whose variation is between  $37.2\%$  (at 7:30 a.m.) and  $64.0\%$  (at 3:30 p.m.);
- Wind speed, whose variation is between  $6.5$  and  $18.1$  m/s.

#### 3.2. Solar Radiation

The solar radiation transmitted by the glazed surfaces that make up the semi-circular greenhouses is shown in Figures 7–9. Solar radiation on the transparent surfaces of semi-circular greenhouse number 5 is shown in Figure 7; solar radiation on the transparent surfaces of semi-circular greenhouse number 6 is shown in Figure 8; and solar radiation on the transparent surfaces of semi-circular greenhouse number 7 is shown in Figure 9.

The solar radiation transmitted on the transparent surfaces of semi-circular greenhouse number 5, which faces northeast, is observed during the morning until around 2 p.m. On the northernmost surfaces, the intensity of solar radiation is low, reaching its maximum before 8 a.m. (below  $6000$  W). On the other hand, on surfaces further east, the intensity of solar radiation is higher, reaching a value close to  $13,000$  W on surface number 1 (see Figure 6) at around 9 a.m. This greenhouse has a low heat storage potential, meaning that

the contribution of its glazed surfaces to heating the interior space of the greenhouse is essentially between 8 a.m. and 10 a.m.

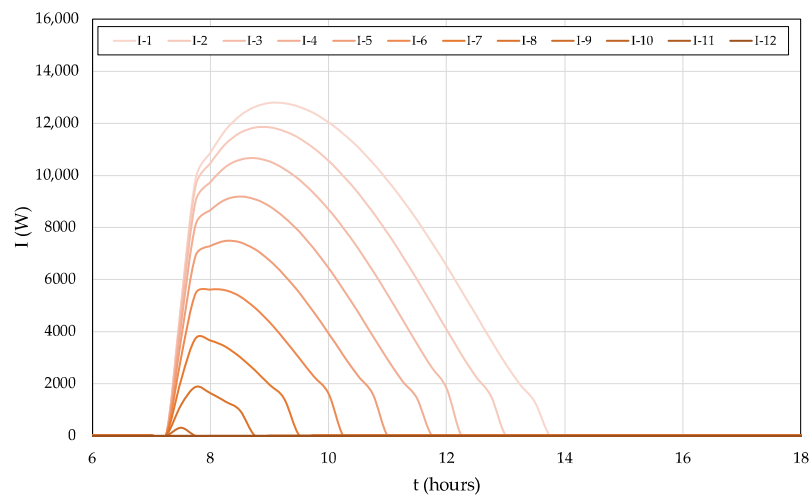


**Figure 7.** Distribution of solar radiation on the transparent surfaces of the semi-circular greenhouse transparent surfaces number 5.

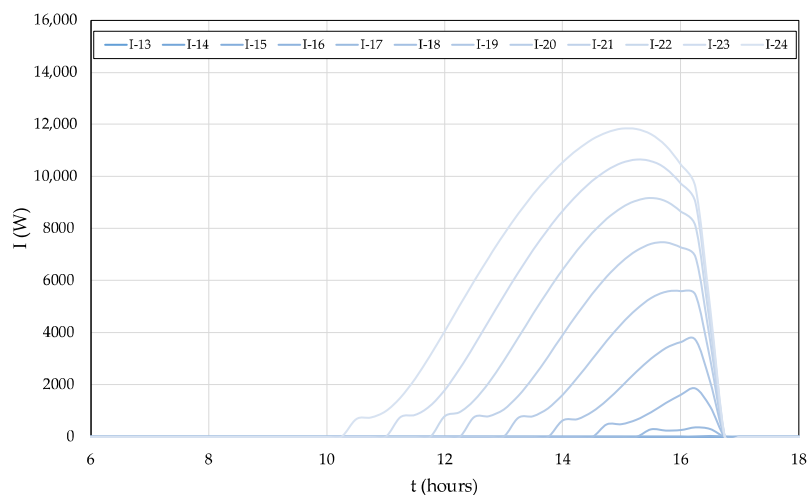


**Figure 8.** Distribution of solar radiation on the transparent surfaces of the semi-circular greenhouse transparent surfaces number 6.

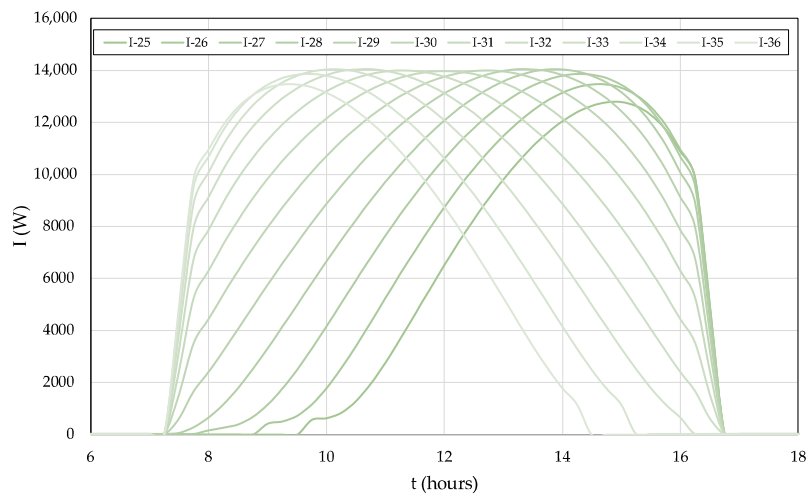


**Figure 9.** Distribution of solar radiation on the transparent surfaces of the semi-circular greenhouse transparent surfaces number 7.

The solar radiation transmitted on the transparent surfaces of semi-circular greenhouse number 6, which faces northwest, is observed mainly during the afternoon until around 4:30 p.m. On the northernmost surfaces, the intensity of solar radiation is low, reaching its maximum around 4 p.m. (below 6000 W). On the other hand, on surfaces further west, the intensity of solar radiation is higher, reaching a value close to 12,000 W on surface number 24 (see Figure 6) at around 3:30 p.m. Like greenhouse number 5, this greenhouse also has a low heat storage potential, meaning that the contribution of its glazed surfaces to heating the interior space of the greenhouse is essentially between 1 p.m. and 4 p.m.

The solar radiation transmitted on the transparent surfaces of semi-circular greenhouse number 6, which faces south, is observed throughout the day. As can be seen in Figure 9, the maximum value of solar radiation intensity is between 13,000 W and 14,000 W for all glazed surfaces of the semi-circular greenhouse 7. Generally speaking, this maximum value occurs on the easternmost surfaces in the morning and on the westernmost surfaces in the afternoon. This greenhouse has a high heating potential for its interior space, practically from sunrise to sunset, meaning the heat stored there can be used effectively to heat the semi-circular auditorium spaces when occupied.

In general, the greatest amount of transmitted solar radiation is found in the semi-circular greenhouse facing south. The semi-circular greenhouse facing northeast only receives some solar radiation in the morning, while the semi-circular greenhouse facing northwest only receives some solar radiation in the afternoon.

### 3.3. Indoor Air Quality

Figure 10 shows the daily evolution of CO<sub>2</sub> concentration calculated numerically within the interior spaces of semi-circular auditoriums 2, 3, and 4. As can be seen, the CO<sub>2</sub> concentration values are below the limit established by the Portuguese standard [44] as acceptable, so it can be seen that IAQ inside auditoriums is acceptable.

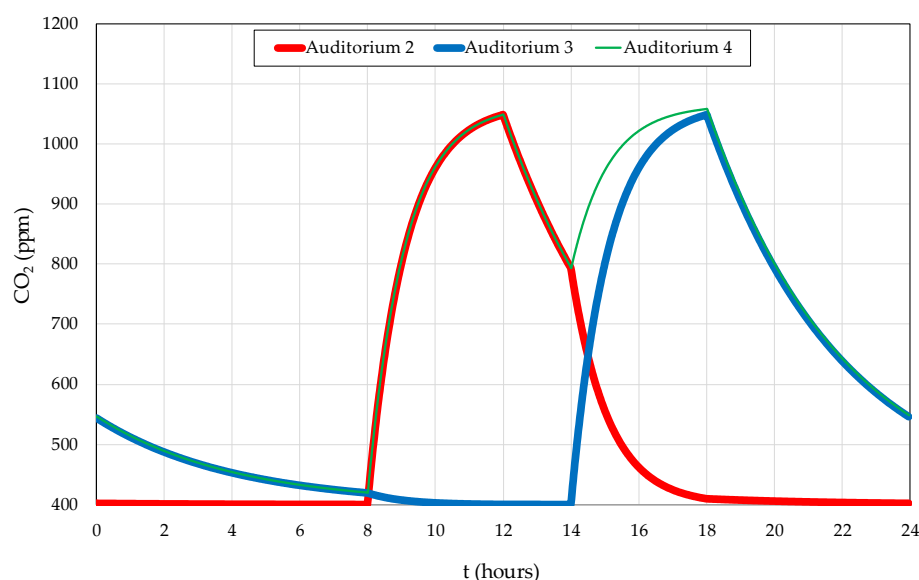


**Figure 10.** CO<sub>2</sub> concentration evolution in the semi-circular auditoriums.

As expected, the highest CO<sub>2</sub> concentration values are obtained when the auditoriums are occupied due to the accumulation of CO<sub>2</sub> produced during the occupants' breathing process. As shown by the obtained results, the airflow rate of 35 m<sup>3</sup>/h per person is adequate to obtain an acceptable level of IAQ during auditorium occupancy; on the other hand, the value of one air change per hour also contributes positively to reducing CO<sub>2</sub> levels in auditoriums when they are unoccupied.

### 3.4. Indoor Air Temperature

Figure 11 shows the internal  $t_a$  evolution in the semi-circular auditoriums 2, 3 and 4 (full line) and in the semi-circular greenhouses 5, 6, and 7 (dashed line).

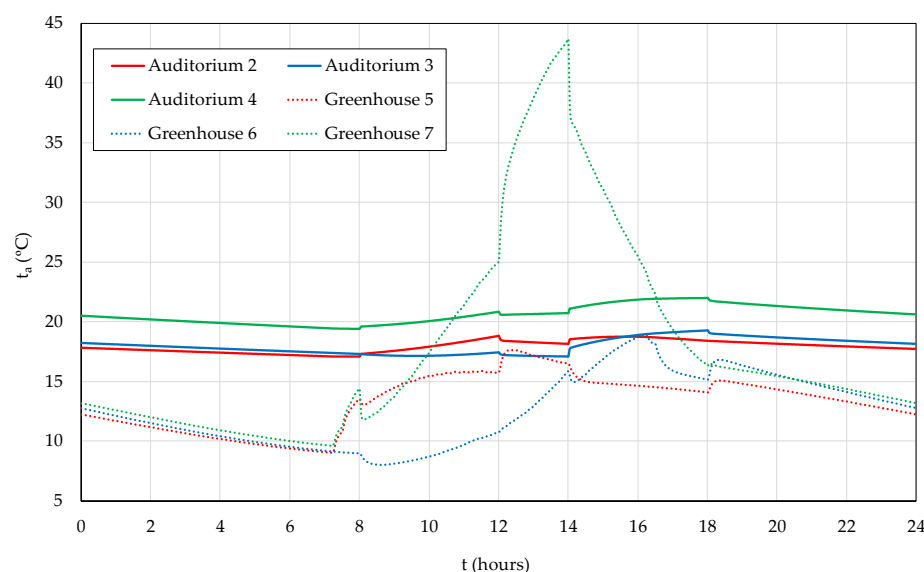


**Figure 11.** Indoor  $t_a$  evolution in the semi-circular auditoriums 2, 3, and 4 (full line) and in the semi-circular greenhouses 5, 6, and 7 (dashed line).

When the auditoriums are occupied, the indoor  $t_a$  varies according to the values presented in Table 3. The results show that  $t_a$  temperatures are higher in auditorium 4, in the morning compared to auditorium 2, and in the afternoon compared to auditorium 3. The positive effect exerted on auditorium 4 by the greenhouse 7 associated with it can be noted. As seen in Figure 6, the ventilation topology shows that the hot air leaves greenhouse 7 first to auditorium 4 before being distributed to the other two auditoriums. It can then be seen that indoor  $t_a$  is greater when the auditoriums are occupied. The temperature values observed there are within or close to the stipulated limit of 19 °C by the Portuguese standard [44] for winter conditions. It is noted that occupants can react positively to the temperatures obtained in the auditoriums with a minor clothing adaptation.

**Table 3.** Variation of  $t_a$  inside auditoriums when occupied.

Auditorium	Morning		Afternoon	
	Minimum $t_a$ (°C)	Maximum $t_a$ (°C)	Minimum $t_a$ (°C)	Maximum $t_a$ (°C)
	8 a.m.	12 a.m.	2 p.m.	6 p.m.
2	17.3	18.9	---	---
3	---	---	17.8	19.1
4	19.4	20.9	20.8	21.9

As is expected in south-facing glazed spaces in the northern hemisphere, the temperature in semi-circular greenhouse 7 facing south presents the highest temperature values, with a peak of 43.5 °C obtained at 2 p.m. In general, the temperature in semi-circular greenhouse 7 is always higher than the temperature in the other two semi-circular greenhouses throughout the day.

In the morning, the indoor  $t_a$  is higher in the semi-circular greenhouse facing north-east, with a variation between 12.3 °C and 15.8 °C, than in the semi-circular greenhouse facing northwest, with a variation between 8.0 °C and 10.8 °C. On the other hand, in the

afternoon the opposite occurs; that is, the indoor  $t_a$  is higher in the semi-circular greenhouse facing northwest, with a variation between 15.0 °C and 18.9 °C, than in the semi-circular greenhouse facing northwest, with a variation between 14.1 °C and 16.3 °C.

### 3.5. Mean Radiant Temperature

Figure 12 shows the  $t_r$  evolution in the semi-circular auditoriums (full line) and the semi-circular greenhouses (dashed line).

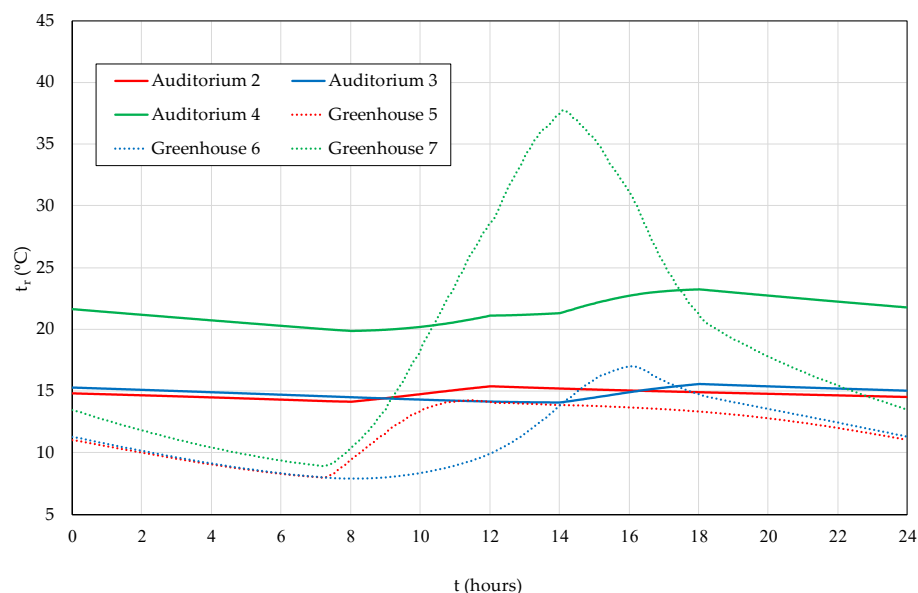


**Figure 12.** Mean radiant temperature,  $t_r$ , evolution in the semi-circular auditoriums (full line) and the semi-circular greenhouses (dashed line).

Regarding the semi-circular greenhouses, the highest  $t_r$  is obtained in the semi-circular greenhouse facing south, space number 7. The  $t_r$  in the northeast semi-circular auditorium, space number 5, is higher than the  $t_r$  in the northwest, space number 6, in the morning. The opposite situation occurs in the afternoon.

Regarding the semi-circular auditoriums, the highest  $t_r$  is obtained in the semi-circular auditorium facing south, space number 4. The  $t_r$  in the semi-circular auditorium facing northwest, space number 2, is slightly higher than the  $t_r$  in the semi-circular auditorium facing northeast, space number 3.

The  $t_r$  is generally close to the internal  $t_a$ , although some differences were noted. In the semi-circular greenhouse facing south, space number 7, the  $t_r$  is higher than the internal  $t_a$  when the space is occupied, whether in the morning or the afternoon. In the semi-circular greenhouses facing northeast, space number 5, and northwest, space number 6, the internal  $t_a$  is higher than  $t_r$ . This fact is due to these semi-circular greenhouses being used for their heating. The semi-circular greenhouse facing south, space number 7, subject to air renewal, is used to heat the air in the semi-circular auditoriums. Therefore, in the two spaces, numbers 5 and 6, the internal  $t_a$  has a greater contribution to the calculation of the PMV index, while in space number 7 the opposite occurs.

In the semi-circular auditoriums facing northwest, space number 2, and northeast, space number 3, the internal  $t_a$  is lower than the  $t_r$ . The  $t_r$  is slightly higher than the internal  $t_a$  in the semi-circular auditorium facing south, space number 4. Such is due to the surrounding surfaces of the semi-circular auditorium facing south, space number 4, being heated directly by solar radiation.

### 3.6. Predicted Mean Vote

The PMV evolution in the semi-circular auditoriums is presented in Figure 13.

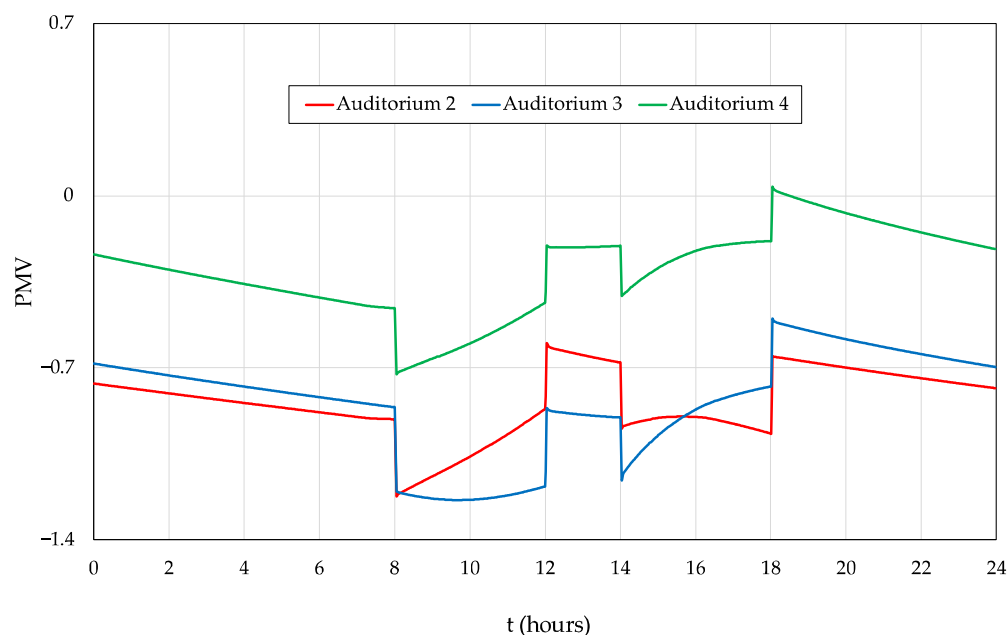


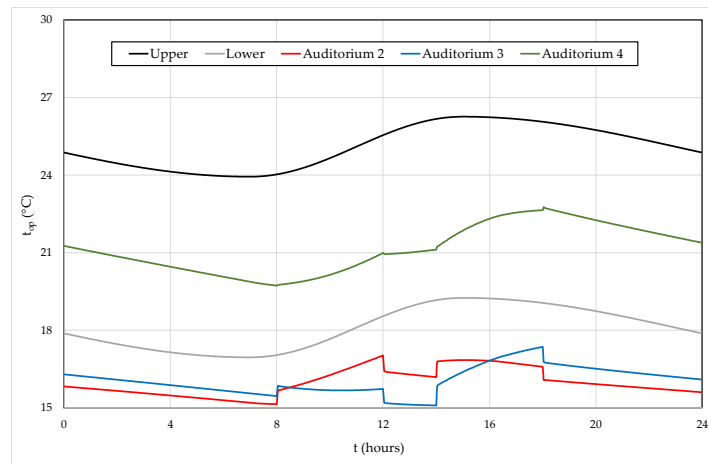
**Figure 13.** PMV evolution in the semi-circular auditoriums.

As spaces are occupied, due to the heat naturally produced by people, the level of indoor  $t_a$  will increase and, therefore, contribute to an increase in the PMV index. Thus, due to occupation, the PMV level increases in the following spaces: in the semi-circular auditorium facing south in the morning and in the afternoon, in the semi-circular auditorium facing northeast in the morning, and in the semi-circular auditorium facing northwest in the afternoon. The PMV index is higher in the semi-circular auditorium facing south than in the semi-circular auditoriums facing northeast and northwest.

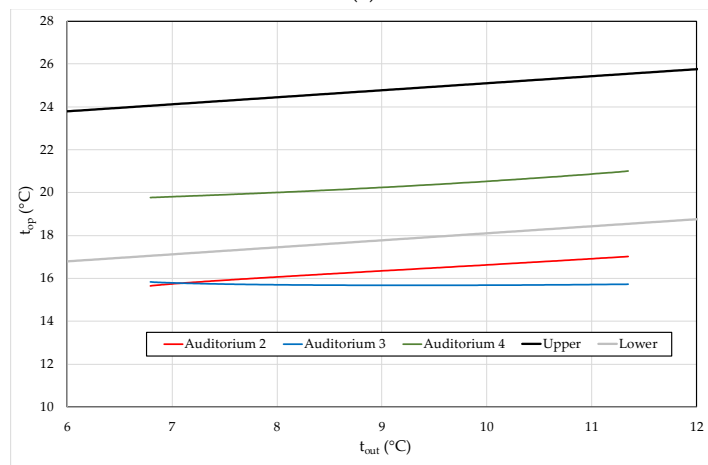
The TC level in the semi-circular auditorium facing south is acceptable all day in line with Category C of the ISO 7730 [45]. The TC level in the semi-circular auditoriums facing northeast and northwest is near the acceptable value when the space is occupied. In these two auditoriums, occupants can achieve TC conditions with some adaptation, for example, by wearing a jacket or with the support of an active heating system that eliminates the difference observed when using only the passive system. However, energy consumption will always be lower than if only the active heating system were used.

### 3.7. Operative Temperature

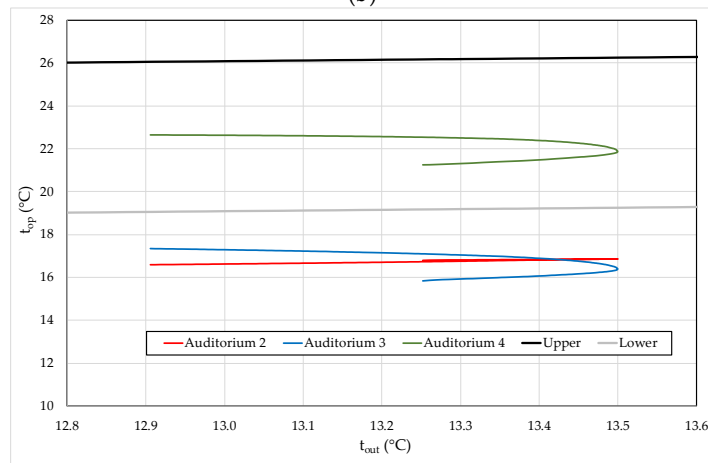
The results obtained from the  $t_{op}$  in the semi-circular auditoriums and the upper and lower  $t_{op}$  limits (as defined in [40]) in ventilated spaces are presented in Figure 14. Figure 14a shows the evolution of the  $t_{op}$  obtained throughout the day, while Figure 14b and 14c show the  $t_{op}$  as a function of the mean outside temperature ( $t_{out}$ ) obtained in the auditoriums during their occupancy period during morning and afternoon, respectively. Figure 14a can be used to calculate, during the day, the comfort level and compared  $T_{op}$  with the PMV results presented in Figure 13. Figure 14b shows groups of points justified by the fact that during this morning period we have essentially linear evolutions of  $t_{out}$  and  $t_r$ . Figure 14c shows the results obtained of the  $T_{op}$  during the afternoon with a curvilinear arrangement, justified by the fact that during this afternoon period we see an inflection in the variation of  $t_{out}$  as a function of time.



(a)



(b)



(c)

**Figure 14.** (a) Evolution of  $t_{op}$  in the semi-circular auditoriums; (b)  $t_{op}$  in function of mean outside temperature  $t_{out}$  obtained when the auditoriums are occupied during the morning [40]; (c)  $t_{op}$  in function of mean outside temperature  $t_{out}$  obtained when the auditoriums are occupied during the afternoon [40]. The upper and lower limits of  $t_{op}$  are defined as presented in Category II of ISO 17772 [40].

The results show that only the  $t_{op}$  of auditorium 4 is located in the adaptive comfort zone (as defined for Category II of ISO 17772 [40]). In auditoriums 2 and 3, the  $t_{op}$  is slightly below the lower limit, indicating that these spaces are uncomfortable because they are slightly cold.

Finally, the conclusions obtained from the analysis of the  $t_{op}$  results are similar to those obtained from the analysis of the PMV results.

#### 4. Conclusions

In this work, an implementation of a ventilation system was proposed for a type of university building with a circular structure, consisting of auditoriums surrounded, throughout their perimeter, by a glazed space. This space could function as a greenhouse where the air from the exterior environment will be previously heated by solar radiation on the glass surfaces before being supplied to the occupied auditoriums. Thermal energy is produced in the surrounding circular greenhouses by the accumulation of radiative heat. The transport of thermal energy between these spaces and the auditorium is performed by the forced air that circulates in the ducts of the ventilation system that connects these spaces. This phenomenon results in a ventilation system that uses the accumulation of hot air stored in a passively heated space. The performance of this ventilation system was evaluated by numerically analyzing its contribution to establishing acceptable TC conditions for occupants also maintaining good IAQ conditions.

Regarding transmitted solar radiation, the highest value is obtained in the semi-circular greenhouse facing south. Semi-circular greenhouses facing northeast and northwest receive significant solar radiation only in the morning and afternoon, respectively.

Using energy transportation from the semi-circular greenhouse to the semi-circular auditorium, the internal ventilation improves the IAQ and the TC level. Due to the higher level, the internal occupation level increases the TC level and reduces the IAQ. However, the ventilation used in the work is sufficient to obtain acceptable IAQ in the occupied spaces.

The indoor  $t_a$  is highest in the semi-circular auditorium when the space is occupied, and the indoor  $t_a$  is highest in the semi-circular greenhouse facing south. In the morning, the indoor  $t_a$  is higher in the semi-circular greenhouse facing northeast than in the semi-circular greenhouse facing northwest. In the afternoon the opposite situation occurs.

In the semi-circular greenhouse facing south, the  $t_r$  is higher than the internal  $t_a$  when the space is occupied. The internal  $t_a$  is higher than  $t_r$  in the semi-circular greenhouses facing northwest and northwest. In the semi-circular auditoriums facing northwest and northeast, the internal  $t_a$  is lower than the  $t_r$ . In the semi-circular auditorium facing south, the  $t_r$  is slightly higher than the internal  $t_a$ .

The semi-circular greenhouse facing south and the occupation level used in the morning and afternoon are sufficient to guarantee acceptable TC conditions in the semi-circular auditory facing south through negative values of the PMV index. However, the semi-circular greenhouse facing south and the occupation level, used in the morning (in the auditorium facing northeast) and in the afternoon (in the semi-circular auditorium facing northwest), are only sufficient to guarantee TC conditions near acceptable thermal conditions in the semi-circular auditoriums facing northeast and northwest. Similar conclusions are also obtained from the analysis of the  $t_{op}$  in ventilated spaces results.

Therefore, it can be concluded that, in the winter season, this ventilation system can contribute to energy savings in this type of building, an inherent advantage of using a well-designed passive heating system, by avoiding the consumption of electrical energy when using HVAC systems connected to the electrical grid, with adequate or close to TC levels and with an IAQ within the recommended limits. However, there are some limitations: the study was carried out under clear sky conditions and for a specific day of the year, so attention must be paid to the reduction in the level of solar radiation on days with the presence of clouds and the reduction in the level of outside air temperature on colder days.

Regarding work to be developed in the future, the application of this type of methodology will be studied in summer conditions using energy also from renewable sources. This type of methodology will make it possible to design the construction of circular auditoriums or buildings with similar geometry, capable of providing suitable conditions of thermal comfort and indoor air quality throughout the year, using renewable energy sources.

**Author Contributions:** E.C., J.G., M.I.C., M.C., M.M.L. and H.A. contributed equally to the design of the work, numerical simulation, analysis of results, writing and review of the manuscript. All authors have read and agreed to the published version of the manuscript.

**Funding:** The authors would like to acknowledge the project SAICT-ALG/39586/2018, DOI 10.54499/SAICT-ALG/39586/2018, from the Algarve Regional Operational Program (CRESC Algarve 2020), under the PORTUGAL 2020 Partnership Agreement, through the European Regional Development Fund (ERDF) and the National Science and Technology Foundation (FCT). The authors also would like to acknowledge the project UIDB/50022/2020, DOI 54499/UIDB/50022/2020, under the National Science and Technology Foundation (FCT).

**Data Availability Statement:** The original contributions presented in this study are included in the article.

**Conflicts of Interest:** The authors declare no conflicts of interest.

## Nomenclature

### Abbreviations

BTR	building thermal response;
CAD	computer-aided design;
CAG	circular auditorium geometry;
CGS	green glass space;
HVAC	heating, ventilation, and air-conditioning
IAQ	indoor air quality;
PMV	predicted mean vote;
PPD	predicted percentage of dissatisfied people;
TC	thermal comfort;

### Symbols

CO <sub>2</sub>	carbon dioxide concentration (ppm);
RH	relative humidity (%);
t	time (h);
t <sub>a</sub>	air temperature (°C);
t <sub>op</sub>	operative temperature in ventilated spaces (°C);
t <sub>out</sub>	mean outside temperature (°C);
t <sub>r</sub>	mean radiant temperature (°C);
v <sub>a</sub>	relative air velocity (m/s).

## References

1. Yuan, J.; Jiao, Z.; Xiao, X.; Emura, K.; Farnham, C. Impact of future climate change on energy consumption in residential buildings: A case study for representative cities in Japan. *Energy Rep.* **2024**, *11*, 1675–1692. [[CrossRef](#)]
2. Wehrli, K.; Sidler, F.; Gubler, S.; Settembrini, G.; Koschenz, M.; Irigoyen, S.; Kotlarski, S.; Fischer, A.; Zweifel, G. Building design in a changing climate—Future Swiss reference years for building simulations. *Clim. Serv.* **2024**, *34*, 100448. [[CrossRef](#)]
3. Yang, L.; Yan, H.; Lam, J. Thermal comfort and building energy consumption implications—a review. *Appl. Energy* **2014**, *115*, 164–173. [[CrossRef](#)]
4. Soares, N.; Bastos, J.; Pereira, L.; Soares, A.; Amaral, A.; Asadi, E.; Rodrigues, E.; Lamas, F.; Monteiro, H.; Lopes, M.; et al. A review on current advances in the energy and environmental performance of buildings towards a more sustainable built environment. *Renew. Sustain. Energy Rev.* **2017**, *77*, 845–860. [[CrossRef](#)]

5. Terés-Zubiaga, J.; Bolliger, R.; Almeida, M.; Barbosa, R.; Rose, J.; Thomsen, K.; Montero, E.; Briones-Llorente, R. Cost-effective building renovation at district level combining energy efficiency & renewables—Methodology assessment proposed in IEA EBC Annex 75 and a demonstration case study. *Energy Build.* **2020**, *224*, 110280.
6. Liang, C.; Li, X.; Shao, X.; Li, B. Numerical analysis of the methods for reducing the energy use of air-conditioning systems in non-uniform indoor environments. *Build. Environ.* **2020**, *167*, 106442. [[CrossRef](#)]
7. Barone, G.; Buonomano, A.; Forzano, C.; Giuzio, G.; Palombo, A.; Russo, G. A new thermal comfort model based on physiological parameters for the smart design and control of energy-efficient HVAC systems. *Renew. Sustain. Energy Rev.* **2023**, *176*, 113015. [[CrossRef](#)]
8. Attia, S.; Kurnitski, J.; Kosiniski, P.; Borodinecs, A.; Belafi, Z.; István, K.; Krstic, H.; Moldovan, M.; Visa, I.; Mihailov, N.; et al. Overview and future challenges of nearly zero-energy building (nZEB) design in Eastern Europe. *Energy Build.* **2022**, *267*, 112165. [[CrossRef](#)]
9. Borowski, M. Hotel Adapted to the Requirements of an nZEB Building—Thermal Energy Performance and Assessment of Energy Retrofit Plan. *Energies* **2022**, *15*, 6332. [[CrossRef](#)]
10. Jaysawal, R.; Chakraborty, S.; Elangovan, D.; Padmanaban, S. Concept of net zero energy buildings (NZEB)—A literature review. *Clean. Eng. Technol.* **2022**, *11*, 100582. [[CrossRef](#)]
11. Santos-Herrero, J.; Lopez-Guede, J.; Flores-Abascal, I. Modeling, simulation and control tools for nZEB: A state-of-the-art review. *Renew. Sustain. Energy Rev.* **2021**, *142*, 110851. [[CrossRef](#)]
12. Carpino, C.; Loukou, E.; Heiselberg, P.; Arcuri, N. Energy performance gap of a nearly Zero Energy Building (nZEB) in Denmark: The influence of occupancy modelling. *Build. Res. Inf.* **2020**, *48*, 899–921. [[CrossRef](#)]
13. Maierhofer, D.; Rock, M.; Saade, M.; Hoxha, E.; Passer, A. Critical life cycle assessment of the innovative passive nZEB building concept ‘be 2226’ in view of net-zero carbon targets. *Build. Environ.* **2022**, *223*, 109476. [[CrossRef](#)]
14. Masi, R.; Gigante, A.; Vanoli, G. Are nZEB design solutions environmental sustainable? Sensitive analysis for building envelope configurations and photovoltaic integration in different climates. *J. Build. Eng.* **2021**, *39*, 102292. [[CrossRef](#)]
15. Resende, J.; Corvacho, H. The nZEB Requirements for Residential Buildings: An Analysis of Thermal Comfort and Actual Energy Needs in Portuguese Climate. *Sustainability* **2021**, *13*, 8277. [[CrossRef](#)]
16. Xi, C.; Ding, J.; Ren, C.; Wang, J.; Feng, Z.; Cao, S. Green glass space based design for the driven of sustainable cities: A case study. *Sustain. Cities Soc.* **2022**, *80*, 103809. [[CrossRef](#)]
17. Zhang, C.; Xi, C.; Feng, Z.; Wang, J.; Cao, S. Passive design for green buildings by using green glass space and earth air tunnel. *Energy Build.* **2022**, *273*, 112367. [[CrossRef](#)]
18. Huang, Y.; Niu, J.; Chung, T. Comprehensive analysis on thermal and daylighting performance of glazing and shading designs on office building envelope in cooling-dominant climates. *Appl. Energy* **2014**, *134*, 215–228. [[CrossRef](#)]
19. Bellia, L.; Falco, F.; Minichiello, F. Effects of solar shading devices on energy requirements of standalone office buildings for Italian climates. *Appl. Therm. Eng.* **2013**, *54*, 190–201. [[CrossRef](#)]
20. Kumar, K.; Saboor, S.; Kumar, V.; Kim, K.; Babu, A. Experimental and theoretical studies of various solar control window glasses for the reduction of cooling and heating loads in buildings across different climatic regions. *Energy Build.* **2018**, *173*, 326–336. [[CrossRef](#)]
21. Cholewa, T.; Malec, A.; Siuta-Olcha, A.; Smolarz, A.; Muryjas, P.; Wolszczak, P.; Guz, Ł.; Dudzińska, M.R.; Łygas, K. On the Influence of Solar Radiation on Heat Delivered to Buildings for Heating. *Energies* **2021**, *14*, 851. [[CrossRef](#)]
22. Liu, X.; Gou, Z. Occupant-centric HVAC and window control: A reinforcement learning model for enhancing indoor thermal comfort and energy efficiency. *Build. Environ.* **2024**, *250*, 111197. [[CrossRef](#)]
23. Wang, L.; Wang, Y.; Fei, F.; Yao, W.; Sun, L. Study on winter thermal environment characteristics and thermal comfort of university classrooms in cold regions of China. *Energy Build.* **2023**, *291*, 113126. [[CrossRef](#)]
24. Hama, S.; Kumar, P.; Tiwari, A.; Wang, Y.; Linden, P. The underpinning factors affecting the classroom air quality, thermal comfort and ventilation in 30 classrooms of primary schools in London. *Environ. Res.* **2023**, *236*, 116863. [[CrossRef](#)] [[PubMed](#)]
25. Alghamdi, S.; Tang, W.; Kanjanabootra, S.; Alterman, D. Field investigations on thermal comfort in university classrooms in New South Wales, Australia. *Energy Rep.* **2023**, *9*, 63–71. [[CrossRef](#)]
26. Pelzer, S.; Aspöck, L.; Schröder, D.; Vorländer, M. Integrating Real-Time Room Acoustics Simulation into a CAD Modeling Software to Enhance the Architectural Design Process. *Buildings* **2014**, *4*, 113–138. [[CrossRef](#)]
27. Aish, R.; Vuren, J.; Walmsley, M. Integrated CAD development for building services engineering. *Comput. Aided Des.* **1985**, *17*, 179–190. [[CrossRef](#)]
28. Jablonska, J.; Czajka, R. CAD Tools and Computing in Architectural and Urban Acoustics. *Buildings* **2021**, *11*, 235. [[CrossRef](#)]
29. Touati, K.; Benzaama, M.-H.; El Mendili, Y.; Le Guern, M.; Streiff, F.; Goodhew, S. Indoor Air Quality in Cob Buildings: In Situ Studies and Artificial Neural Network Modeling. *Buildings* **2023**, *13*, 2892. [[CrossRef](#)]
30. Tam, C.; Zhao, Y.; Liao, Z.; Zhao, L. Mitigation Strategies for Overheating and High Carbon Dioxide Concentration within Institutional Buildings: A Case Study in Toronto, Canada. *Buildings* **2020**, *10*, 124. [[CrossRef](#)]

31. Miao, S.; Gangoellis, M.; Tejedor, B. Data-driven model for predicting indoor air quality and thermal comfort levels in naturally ventilated educational buildings using easily accessible data for schools. *J. Build. Eng.* **2023**, *80*, 108001. [[CrossRef](#)]
32. Pei, G.; Freihaut, J.; Rim, D. Long-term application of low-cost sensors for monitoring indoor air quality and particle dynamics in a commercial building. *J. Build. Eng.* **2023**, *79*, 107774. [[CrossRef](#)]
33. Jahanbin, A.; Semprini, G. On the optimisation of age of the air in the breathing zone of floor heating systems: The role of ventilation design. *Energy Built Environ.* **2024**, *5*, 130–142. [[CrossRef](#)]
34. Tognon, G.; Marigo, M.; Carli, M.; Zarrella, A. Mechanical, natural and hybrid ventilation systems in different building types: Energy and indoor air quality analysis. *J. Build. Eng.* **2023**, *76*, 107060. [[CrossRef](#)]
35. Ng, L.; Musser, A.; Persily, A.; Emmerich, S. Multizone airflow models for calculating infiltration rates in commercial reference buildings. *Energy Build.* **2013**, *58*, 11–18. [[CrossRef](#)]
36. Choi, K.; Park, S.; Joe, J.; Kim, S.; Jo, J.; Kim, E.; Cho, Y. Review of infiltration and airflow models in building energy simulations for providing guidelines to building energy modelers. *Renew. Sustain. Energy Rev.* **2023**, *181*, 113327. [[CrossRef](#)]
37. Makaveckas, T.; Bliūdžius, R.; Alavočienė, S.; Paukštys, V.; Brazionienė, I. Investigation of Microclimate Parameter Assurance in Schools with Natural Ventilation Systems. *Buildings* **2023**, *13*, 1807. [[CrossRef](#)]
38. McNeill, V.; Corsi, R.; Huffman, J.; King, C.; Klein, R.; Lamore, M.; Maeng, D.; Miller, S.; Ng, N.; Olsiewski, P.; et al. Room-level ventilation in schools and universities. *Atmos. Environ. X* **2022**, *13*, 100152. [[CrossRef](#)]
39. *ANSI/ASHRAE Standard 62-1; Ventilation for Acceptable Indoor Air Quality*. American Society of Heating, Refrigerating and Air-Conditioning Engineers: Atlanta, GA, USA, 2022.
40. *ISO 17772-1:2017; Energy Performance of Buildings—Indoor Environmental Quality—Part 1: Indoor Environmental Input Parameters for the Design and Assessment of Energy Performance of Buildings*. ISO: Geneva, Switzerland, 2017.
41. *ISO/TR 17772-2; Energy Performance of Buildings—Overall Energy Performance Assessment Procedures—Part 2: Guideline for Using Indoor Environmental Input Parameters for the Design and Assessment of Energy Performance of Buildings (Technical Report)*. ISO: Geneva, Switzerland, 2018.
42. *EN 16798-1; Energy Performance of Buildings—Ventilation for Buildings—Part 1: Indoor Environmental Input Parameters for Design and Assessment of Energy Performance of Buildings Addressing Indoor Air Quality, Thermal Environment, Lighting and Acoustics—Module M1-6*. CEN: Brussels, Belgium, 2019.
43. *DS/CEN/TR 16798-2:2019; Energy Performance of Buildings—Ventilation for Buildings—Part 2: Interpretation of the Requirements in EN 16798-1—Indoor Environmental Input Parameters for Design and Assessment of Energy Performance of Buildings Addressing Indoor Air Quality, Thermal Environment, Lighting and Acoustics (Module M1-6)*. Danish Standard Association: Nordhavn, Denmark, 2019.
44. *Portaria 353-A/2013; Regulamento de Desempenho Energético dos Edifícios de Comércio e Serviços (RECS)—Requisitos de Ventilação e Qualidade do Ar Interior—Portaria no 353-A/2013 de 4 de Dezembro. 1ª Série 245. Diário República: Lisboa, Portugal, 2013; pp. 6644-(2)–6644-(9). (In Portuguese)*
45. *ISO 7730:2005; Ergonomics of the Thermal Environment Analytical Determination and Interpretation of Thermal Comfort Using Calculation of the PMV and PPD Indices and Local Thermal Comfort Criteria*. ISO: Geneva, Switzerland, 2005.
46. *ANSI/ASHRAE Standard-55; Thermal Environmental Conditions for Human Occupancy*. American Society of Heating, Refrigerating and Air-Conditioning Engineers: Atlanta, GA, USA, 2017.
47. Fanger, P. *Thermal Comfort: Analysis and Applications in Environmental Engineering*; Danish Technical Press: Copenhagen, Denmark, 1970.
48. Zomorodian, Z.; Tahsildoost, M.; Hafezi, M. Thermal comfort in educational buildings: A review article. *Renew. Sustain. Energy Rev.* **2016**, *59*, 895–906. [[CrossRef](#)]
49. Park, J.; Choi, H.; Kim, D.; Kim, T. Development of novel PMV-based HVAC control strategies using a mean radiant temperature prediction model by machine learning in Kuwaiti climate. *Build. Environ.* **2021**, *206*, 108357. [[CrossRef](#)]
50. Kim, J.; Yoon, S. Virtual PMV sensor towards smart thermostats: Comparison of modeling approaches using intrusive data. *Energy Build.* **2023**, *301*, 113695. [[CrossRef](#)]
51. Choi, F.; Yun, J.; Choi, Y.; Seo, M.; Moon, J. Impact of thermal control by real-time PMV using estimated occupants personal factors of metabolic rate and clothing insulation. *Energy Build.* **2024**, *307*, 113976. [[CrossRef](#)]
52. Gao, J.; Wang, Y.; Wargocki, P. Comparative analysis of modified PMV models and SET models to predict human thermal sensation in naturally ventilated buildings. *Build. Environ.* **2015**, *92*, 200–208. [[CrossRef](#)]
53. Hoz-Torres, M.; Aguilar, A.; Ruiz, D.; Martínez-Aires, M. An investigation of indoor thermal environments and thermal comfort in naturally ventilated educational buildings. *J. Build. Eng.* **2024**, *84*, 108677. [[CrossRef](#)]
54. Alfano, F.; Ianniello, E.; Palella, B. PMV-PPD and acceptability in naturally ventilated schools. *Build. Environ.* **2013**, *67*, 129–137. [[CrossRef](#)]
55. Takahashi, Y.; Nomoto, A.; Yoda, S.; Hisayama, R.; Ogata, M.; Ozeki, Y.; Tanabe, S. Thermoregulation Model JOS-3 With New Open Source Code. *Energy Build.* **2021**, *231*, 110575. [[CrossRef](#)]

56. Alfano, F.; Palella, B.; Riccio, G. THERMODE 2023: Formulation and Validation of a New Thermo-physiological Model for Moderate Environments. *Build. Environ.* **2024**, *252*, 111272. [[CrossRef](#)]
57. Conceição, E.; Gomes, J.; Lúcio, M.; Awbi, H. Development of a Double Skin Facade System Applied in a Virtual Occupied Chamber. *Inventions* **2021**, *6*, 17. [[CrossRef](#)]
58. Conceição, E.; Lúcio, M. Numerical Simulation of the Application of Solar Radiant Systems, Internal Airflow and Occupants' Presence in the Improvement of Comfort in Winter Conditions. *Buildings* **2016**, *6*, 38. [[CrossRef](#)]
59. Picallo-Perez, A.; Sala-Lizarraga, J.; Portillo-Valdes, L. Development of a tool based on thermoeconomics for control and diagnosis building thermal facilities. *Energy* **2022**, *239 Pt D*, 122304. [[CrossRef](#)]
60. Fawwaz Alrebei, O.; Obeidat, L.M.; Ma'bdeh, S.N.; Kaouri, K.; Al-Radaideh, T.; Amhamed, A.I. Window-Windcatcher for Enhanced Thermal Comfort, Natural Ventilation and Reduced COVID-19 Transmission. *Buildings* **2022**, *12*, 791. [[CrossRef](#)]
61. Diz-Mellado, E.; Ruiz-Pardo, A.; Rivera-Gómez, C.; Flor, F.; Galán-Marín, C. Unravelling the impact of courtyard geometry on cooling energy consumption in buildings. *Build. Environ.* **2023**, *237*, 110349. [[CrossRef](#)]
62. Global Solar Atlas. Available online: <https://globalsolaratlas.info/map?c=36.712467,-9.191763,8&m=site> (accessed on 22 February 2024).
63. Conceição, M.I.; Conceição, E.; Lúcio, M.; Gomes, J.; Awbi, H. Application of Semi-Circular Double-Skin Facades in Auditoriums in Winter Conditions. *Inventions* **2023**, *8*, 60. [[CrossRef](#)]
64. Conceição, E.; Lúcio, M. Numerical simulation of passive and active solar strategies in buildings with complex topology. *Build. Simul.* **2010**, *3*, 245–261. [[CrossRef](#)]
65. Conceição, E.; Gomes, J.; Awbi, H. Influence of the Airflow in a Solar Passive Building on the Indoor Air Quality and Thermal Comfort Levels. *Atmosphere* **2019**, *10*, 766. [[CrossRef](#)]
66. Alfano, F.; Pepe, D.; Riccio, G.; Vio, M.; Palella, B. On the effects of the mean radiant temperature evaluation in the assessment of thermal comfort by dynamic energy simulation tools. *Build. Environ.* **2023**, *236*, 110254. [[CrossRef](#)]
67. Lee, D.; Jo, J. Measuring and implementing mean radiant temperature in buildings: Technical review. *Renew. Sustain. Energy Rev.* **2025**, *207*, 114908. [[CrossRef](#)]
68. Haiying, W.; Fengming, Z.; Jiankai, L.; Hang, M.; Huxiang, L. Effects of different zoning thermostat controls on thermal comfort and cooling energy consumption in reading rooms of a library. *Energy* **2024**, *292*, 130507. [[CrossRef](#)]
69. Khovalyg, D.; Kazanci, O.; Halvorsen, H.; Gundlach, I.; Bahnfleth, W.; Toftum, J.; Olesen, B. Critical review of standards for indoor thermal environment and air quality. *Energy Build.* **2020**, *213*, 109819. [[CrossRef](#)]

**Disclaimer/Publisher's Note:** The statements, opinions and data contained in all publications are solely those of the individual author(s) and contributor(s) and not of MDPI and/or the editor(s). MDPI and/or the editor(s) disclaim responsibility for any injury to people or property resulting from any ideas, methods, instructions or products referred to in the content.